# Electronic Absorption and Resonance Raman Spectroscopy from Ab Initio Quantum Molecular Dynamics

**M. Ben-Nun* and Todd J. Martínez**

*Department of Chemistry and The Beckman Institute, University of Illinois, Urbana, Illinois 61801*

*Received: June 29, 1999; In Final Form: September 29, 1999*

The absorption and resonance Raman excitation profiles of ethylene following $\pi \rightarrow \pi^*$ excitation and taking full account of anharmonicity and Duschinsky rotation effects are calculated from first principles molecular dynamics using the ab initio multiple spawning (AIMS) method and a correlation function approach. The AIMS method solves the nuclear and electronic Schrödinger equations simultaneously and it associates a unique nuclear wave function with each electronic state. The computed absorption spectrum has a full width at half maximum of $9800 \pm 1300$ cm$^{-1}$ (in agreement with the experimental value, 9500 cm$^{-1}$) and a high-frequency structure spaced by $800 \pm 10$ cm$^{-1}$, attributed to C═C stretching. The resonance Raman excitation profile exhibits fundamental activity in all totally symmetric modes with the C═C stretching mode being the most dominant. In addition, overtone activity is observed in the torsional motion, out-of-plane wagging motions and the out-of-plane rocking motions. This activity is consistent with the observation that the first excited state is twisted and one of the $CH_2$ groups is pyramidalized. The coordinate dependence of the electronic transition dipole is investigated, and we find that it depends very strongly on the torsional coordinate and less so on the pyramidalization and C═C stretching coordinates. However, within the approximations used in this paper this dependence does not influence the spectra significantly and the Condon approximation is quite accurate.

## I. Introduction

The electronic absorption and resonance Raman spectra of a molecule provide valuable information about excited state potential energy surfaces and the molecular dynamics which ensues on these surfaces. Unfortunately, this information is encoded through time integration, sometimes making detailed interpretation treacherous. A case in point here is the absorption spectrum of ethylene, where debate about the correct assignment still continues.[1−7] Ideally, one would like to be able to compute spectra directly for large molecules and condensed phases without a priori assumptions both in order to interpret the spectra and also to verify our understanding of molecular potential energy surfaces (PESs). Kent Wilson envisioned this goal early on and made seminal contributions, showing how molecular dynamics could be used to complete the connection between PESs and experimental spectra from the gas phase through to condensed phases.[8,9]

With the establishment of analytic gradient techniques,[10,11] ab initio quantum chemistry has become a valuable tool in the assignment and interpretation of spectra.[7,12−14] However, the resulting stick spectra often neglect anharmonicity effects and are unable to address the line shapes that reflect the underlying molecular dynamics. Extracting the full information present in the spectrum requires solution of the nuclear Schrödinger equation on the given PESs. It is now quite clear that time-dependent approaches are most efficient for this purpose, and in many ways they are also more easily interpreted than the alternative time-independent approach.[15,16]

The simulation of these spectra via numerically exact propagation of nuclear wave functions on assumed PESs has become a routine procedure for up to five degrees of freedom.[17−28] However, the restricted dimensionality forces investigation of small molecules or the assumption that only a reduced number of modes are relevant to the spectrum. By using approximate dynamical techniques (which in some cases may be practically exact), larger molecules can be treated without reduced dimensionality assumptions. An impressive recent example computes the absorption spectrum of pyrazine[29] explicitly including all 24 vibrational modes and using harmonic potential energy surfaces fit to ab initio data.

The problem of generating electronic spectra is naturally divided into two parts: the computation of ground and excited state PESs and the subsequent quantum nuclear dynamics. A satisfactory solution requires that both issues be adequately addressed. Because each of the individual problems may already be quite challenging, it has been customary to emphasize one over the other. For example, high-level ab initio calculations have been used to generate harmonic approximations to the PESs for which the Franck−Condon integrals may be solved exactly and numerically exact quantum dynamics has been employed in reduced dimensionality on model PESs. These studies have been very informative, but theoretical and computational advances make it possible to explore a more balanced approach.

The conventional way of generating electronic spectra decomposes the problem into two parts that are done sequentially: fitting of empirical functional forms to ab initio data and subsequent solution of the nuclear dynamics on these empirical PESs. A more elegant approach would address both aspects simultaneously, generating the required PESs via solution of the electronic Schrödinger equation when and where the nuclear dynamics dictates. Ab initio molecular dynamics[30−34] is designed for precisely this purpose. However, until our recent work,[35−41] these methods have been confined to the realm of

10.1021/jp992197r CCC: $18.00 © 1999 American Chemical Society
Published on Web 11/13/1999

classical molecular dynamics, precluding the description of dynamics on multiple electronic states and/or tunneling effects. We have introduced and developed the ab initio multiple spawning (AIMS) approach which includes quantum mechanical effects on the nuclear dynamics in a way that is amenable to "on-the-fly" generation of PESs via ab initio quantum chemistry.

In the following, we apply AIMS to the computation of electronic absorption and resonance Raman spectra of ethylene. This work represents the first attempt to compute electronic spectra directly from first principles molecular dynamics, without intermediate fitting of ab initio PESs to empirical functional forms. Electronic spectra are a natural application of AIMS because they are often largely determined by short-time (<100 fs) dynamical information. The expense of generating PESs "on-the-fly" makes long propagation times difficult in AIMS, and the dynamical approximations that must be made are expected to be most accurate for short-time propagation. The AIMS method treats all degrees of freedom on the same footing and it is possible to include the coordinate dependence of the electronic transition dipole. It has been shown for some one-dimensional models that the latter can have important effects on resonance Raman spectra.[42,43]

There is a long history to studies of the electronic absorption spectrum of ethylene. It was clear from the outset that multiple overlapping bands were present, and Wilkinson and Mulliken assigned these to the $\pi \rightarrow \pi^*$ valence (V) state and Rydberg (R) states.[1] There is a single progression in the V state band of $C_2H_4$, originally assigned to C=C stretching motion.[1] Later investigations questioned this assignment and suggested a purely torsional progression.[3] Foo and Innes[2] agreed with the reassignment based on their spectral study of ethylene isotopomers but suggested a mixture of C=C stretching and torsion. Theoretical studies[44] which predicted that the change in C=C bond length on the excited state was less than 0.1 Å convinced Mulliken[45,46] that torsion dominated the spectrum. The accepted assignment of mixed C=C stretching and torsion was challenged by Siebrand and co-workers,[6] who presented theoretical evidence that there is no visible C=C activity in the spectrum. Subsequently there have been few challenges to the torsional assignment of the progression. However, the very identity of the bands has been recently challenged.[5]

The next section begins with a short review of the full multiple spawning method that forms the cornerstone of our dynamical approach (subsection II.A). We then proceed to discuss the solution of the electronic Schrödinger equation (subsection II.B), nuclear basis set selection (subsection II.C), and the computation of the absorption and resonance Raman excitation profiles (subsection II.D). In section III our theoretical predictions for the absorption and resonance Raman excitation profiles of ethylene (following $\pi \rightarrow \pi^*$ excitation) are presented. When appropriate these predictions are compared with the experimental spectra and we conclude with a discussion in section IV.

## II. Theory

We use the full multiple spawning (FMS) method to describe the quantum nuclear dynamics and to construct the relevant correlation functions whose Fourier transforms are the absorption and resonance Raman excitation profiles. The FMS method provides a description of quantum nuclear dynamics that is tailored to the requirements of ab initio quantum chemistry. This makes ab initio multiple spawning (AIMS) possible, where the electronic and nuclear Schrödinger equations are solved simultaneously. The primary advantages of AIMS are that intermediate fitting of PESs is avoided, bond rearrangement is treated naturally, electronic excited states can be modeled correctly, and intrinsically quantum mechanical effects in the nuclear dynamics are included in an approximate manner. In the work described here, the quantum nuclear dynamics is of particular importance, because the presence of a nuclear wave function allows us to model the spectrum through a correlation function approach. This takes full account of anharmonicity and Duschinsky rotation effects. Furthermore, nonadiabatic effects that could influence the observed spectra by shortening the excited state lifetime are also incorporated. In what follows we provide a brief discussion of the method and we refer the reader to our previous work[35,37,41,47−50] for more details.

**A. Solution of the Nuclear Schrödinger Equation − The Full Multiple Spawning Method.** The FMS method can be viewed as a particular form of wave packet propagation, using an adaptive time-dependent basis set for the nuclear wave function. Classical mechanics is employed to provide a guide for basis set selection and propagation, but ultimately the dynamics is dictated by the solution of the nuclear Schrödinger equation within this basis set. Each basis function in the expansion of the nuclear wave function carries an electronic state label, and the centers of the basis functions obey classical equations of motion under the potential corresponding to the appropriate electronic state. The basis functions are chosen to be of the "frozen Gaussian" form,[51] and the key point is that the classical nature of the time evolution of the basis requires only local quantities − potential gradients at a single nuclear configuration per basis function per time step. Solution of the nuclear Schrödinger equation in the chosen basis requires evaluation of matrix elements that are integrals over the potential energy surface or coupling between potential energy surfaces (diagonal and off-diagonal matrix elements of the Hamiltonian, respectively). A first-order saddle-point (SP) procedure,[49] motivated by the local nature of the nuclear basis functions, is used to evaluate these matrix elements. The concept of spawning refers to the means of adaptively selecting a basis set which is appropriate for the dynamics at hand. In the ideal limit where basis set convergence is reached, the dynamics represents the exact solution of the nuclear Schrödinger equation. At the opposite extreme where the basis set is restricted to a single function, semiclassical Gaussian wave packet dynamics[51] is obtained. In the practically relevant situation where the basis set is of small or intermediate size, the method is expected to be most useful when classical mechanics provides a relevant zeroth order picture. This is often the case in molecules of chemical interest. The frequency with which basis functions are added can be controlled, giving a hierarchy of approximations with increasing accuracy. This is an important aspect of the method because it allows one to investigate whether various observables are converged at a particular level of approximation. Unfortunately, this is not currently possible when the PESs are evaluated "on-the-fly," although we have investigated this possibility for low-dimensional problems with empirical PESs where exact quantum results could be generated for comparison.[35] For the molecule considered in this work, ethylene, the absorption and resonance Raman excitation profiles are fully determined before the onset of nonadiabatic events (through which the excited state molecule quenches back to the ground electronic state, see ref 41). Therefore, we omit any further discussion of the dynamical expansion of the size of the basis set ("spawning") during nonadiabatic events.

**B. Solution of the Electronic Schrödinger Equation.** The solution of the electronic Schrödinger equation must provide at each point in time (i) the potential and force for each nuclear basis function and (ii) the first-order SP approximation to the diagonal and off-diagonal elements of the Hamiltonian matrix. The procedure used to solve the electronic structure problem is motivated by a desire to balance accuracy and expense. As in any investigation of ground and excited states, we require an unbiased treatment. That is, a variational bias toward the ground electronic state must be avoided and the quality of the solution must be similar for all of the desired states. A second requirement is simplification of the computation of the nonadiabatic coupling between electronic states. Within the context of ab initio quantum chemistry, this can be achieved by employing the same set of molecular orbitals to describe the relevant states. These considerations are best addressed by determining the relevant molecular orbitals in a state-averaged approach.[52] In the case of ethylene, these orbitals are the two $\pi$ and $\pi^*$ orbitals. We first determine the "best compromise" relevant orbitals (expanded in a double-$\zeta$ Gaussian basis set[53]) by minimizing an energy expression in which one electron is placed in each of the two relevant orbitals. Once we obtain this state-averaged optimized set of molecular orbitals, we model the state-dependent orbital relaxation using a multireference configuration interaction (MRCI) including single excitations. In the case of ethylene, the two active orbitals and two electrons result in three reference configurations ($\pi\pi$, $\pi\pi^*$, and $\pi^*\pi^*$). Subsequent diagonalization of the CI Hamiltonian matrix gives the desired potential energies and electronic wave functions at each nuclear configuration. Only the two lowest adiabatic electronic states (i.e., ground and first excited) are included in the computation. Thus the dynamics is assumed to be adiabatic with respect to other electronic states.

At each time step and for each nuclear basis function and/or Hamiltonian matrix element, the necessary potential energies, gradients, and/or nonadiabatic couplings are obtained using the procedure outlined above. The derivatives of the PESs (i.e., forces) are obtained numerically using a symmetric finite difference formula with a step-size of 0.005 bohr. A numerical finite-difference procedure is also used to evaluate the nonadiabatic couplings, $\langle \psi_{ground} | {}^{\partial}/_{\partial R} | \psi_{\text{excited}} \rangle$ . Because they were found to have no effect on the very early time ($<$50 fs) dynamics that is the topic of this paper, we refrain from discussing them further.

Finally, a word is in place about the expected accuracy of the PESs and of the absorption and resonance Raman excitation profiles. Even with first-order SP approximations, which reduce the number of potential energy evaluations to $O(n^2)$ per time step, a complete description of the spectroscopy and excited states of ethylene[1-4,46,54-56] is beyond our current computational capabilities. Such a description requires the inclusion of diffuse electronic basis functions because of low-lying Rydberg states.[44,57-64] We do not include such diffuse basis functions in the calculations, and therefore we cannot reproduce their spectroscopic manifestation (the structure at the low energy end of the absorption spectrum, see, for example, ref 4). What we do try to model are those spectroscopic features that arise due to the state with the strongest oscillator strength: the $\pi \rightarrow \pi^*$ (V) excited state. In the future it will be possible to improve the description of other excited states by including diffuse basis functions and by extending the CI to include double excitations. Once such a computation becomes feasible we could try to model these effects by considering the time evolution of a coherent superposition of the different relevant excited states where the initial relative populations are determined by the relevant oscillator strength. In this first attempt to describe spectra from ab initio molecular dynamics we have not done this and instead assume an idealized electronic excitation that accesses only the V state.

**C. Nuclear Basis Set Selection.** Our wave function ansatz takes the width parameter for each Gaussian nuclear basis function to be real and time-independent. Its optimal value is known only for the case of a harmonic potential energy surface:[65] $\alpha = m\omega/2$ where $\omega$ and $m$ are the harmonic frequency and reduced mass, respectively. For the case of a general potential, we view the width as a parameter whose specific value should be both physically reasonable and large enough to ensure the quality of the SP approximation that we use. (The quality of SP approximations deteriorates with extended basis functions in position space, and therefore the width must be large enough to justify these approximations.) Motivated by the result of the harmonic case, we propose (and use in section III) the following physical choice for the width.

Given any polyatomic molecule we first determine the ground state equilibrium geometry, the normal mode frequencies, and the normal mode eigenvectors that provide the transformation between the Cartesian and normal mode coordinate systems. Using the $(3N - 6)$ normal mode frequencies we construct a diagonal $(3N - 6) \times (3N - 6)$, normal mode, "width" matrix. Within the normal mode approximation this is the exact "width" matrix. This matrix is then rotated to a Cartesian coordinate system using the normal mode eigenvectors. The result of this transformation is a $3N \times 3N$ Cartesian "width" matrix whose off-diagonal elements are in general not zero and whose Cartesian components are not equal (i.e., the $x$, $y$, and $z$ components of any atom need not be the same). Our ansatz does not allow for correlation between the Cartesian components of a given basis function, i.e., the Cartesian "width" matrix is assumed diagonal. We also demand invariance with respect to permutation of equivalent particles and rotation of the molecule. These considerations lead us to (i) ignore the off-diagonal elements of the Cartesian width matrix and (ii) average the diagonal ones for each chemical element. The end result is a single value for each element, e.g. carbon, that is the average of the $x$, $y$, and $z$ components of all the same elements. The specific values that we obtain are similar to what one would obtain by considering typical C=C and CH frequencies. For ethylene, we obtain values of 30 bohr$^{-2}$ and 6 bohr$^{-2}$ for C and H, respectively. The same width is used on both surfaces.

We assume that initially only the V state is populated and that the initial conditions on the ground electronic state are such that all normal modes are in their ground vibrational state. A Monte Carlo (MC) procedure is used to sample the initial position and momentum parameters from the appropriate Wigner distribution,[66] and the initial value of the nuclear phase is set to zero. Once the initial position and momentum parameters for all of the nuclear basis functions are selected they are rotated to the Cartesian coordinate system that is used in the actual propagation. The initial values of the complex trajectory amplitudes are chosen so that the wave function reproduces the exact $t = 0$ wave function as well as possible within the given basis set.

**D. Calculation of Absorption and Resonance Raman Excitation Profiles.** The FMS method associates a nuclear wave function with each electronic state, and hence one has direct access to dynamical quantities on each individual state. In this subsection we discuss the computation of the electronic absorption and resonance Raman spectra using the FMS wave function.

The time-dependent expression for the absorption cross section is given by[15,67,68]

$$\sigma_A(\omega_I) = C\omega_I \int_{-\infty}^{+\infty} \langle\phi_i|\phi_i(t)\rangle \exp(i\tilde{\omega}_I t)\mathrm{d}t \qquad (2.1)$$

where

$$\tilde{\omega}_I = \omega_I + \omega_i$$

$$|\phi_i\rangle = \mu(\mathbf{R})|i\rangle$$

$$|\phi_i(t)\rangle = \exp(-i\hat{H}_{ex}t)|\phi_i\rangle \qquad (2.2)$$

In eqs 2.1 and 2.2, $C$ is a constant, $\omega_I$ is the energy of the incident radiation, $\omega_i$ is the zero point energy of the ground electronic state, $|i\rangle$ is the initial (ground state) vibrational wave function, $\mu(\mathbf{R})$ is the (coordinate dependent) electronic transition dipole moment, and $|\phi_i(t)\rangle$ is the ground state wave function (multiplied by the electronic transition dipole) propagated on the excited electronic state. Note that eq 2.1 assumes the validity of the Born−Oppenheimer approximation, i.e., the time evolution of the excited state wave packet is governed by a single PES. This assumption is not always correct both because more than one excited electronic state may be accessed by the electronic excitation and because of avoided and/or true crossings of the excited and ground (and/or other excited) states. In the present case eq 2.1 is sufficient because we assume that only one excited electronic state is accessed, and because the absorption spectrum is fully determined before the onset of nonadiabatic events. In other words, there is a separation of time scales between the time evolution in the Franck−Condon region and the nonadiabatic events that bring the molecule back to the ground electronic state. (We reemphasize that in the actual propagation, section III, we do use the coupled multistate Hamiltonian, but we simplify the notation here because of the separation of time scales that was observed.) We also note that although the electronic transition dipole moment depends on the nuclear coordinates, it is customary to neglect this dependence (Condon approximation). Notable exceptions to this for the case of ethylene are the studies of Petrongolo et al.[61] and Dormans et al.[69] who investigated the torsional dependence of the electronic transition dipole. Within the Condon approximation the computation of the absorption profile requires a Fourier transform of the autocorrelation function which is easily constructed from the FMS wave function. Given our wave function ansatz, the multidimensional integral can be expressed as a weighted sum of products of 3N one-dimensional Gaussian overlap integrals.

We have also investigated the absorption (and resonance Raman, see below) spectrum without the Condon approximation but with the neglect of the commutator between the propagator and the electronic transition dipole, i.e., $\exp(-i\hat{H}_{ex}t)\mu(\mathbf{R})|i\rangle \approx \mu(\mathbf{R})\exp(-i\hat{H}_{ex}t)|i\rangle$, an approximation that is correct to $O(t)$. Since both the initial and the time evolving wave functions are given by a weighted sum of multidimensional Gaussian basis functions, we need to evaluate integrals that are products of nuclear basis functions (of Gaussian form) and the square of the electronic transition dipole, at each point in time. One possibility of including the effect of the nonconstant transition dipole is to expand it in a Taylor series or fit it to an empirical function, e.g., an exponential.[42] In either case, the resulting integrals may be evaluated analytically. As in the case of fitting PESs, this becomes impractical in many dimensions. Hence, we evaluate these integrals using a first-order SP approximation. This is done at each point in time and it requires $O(n_{t=0}n_t)$ calculations where $n_t$ is the number of basis functions used to represent the wave function at time $t$. Computationally, the calculation of the electronic transition dipole is quite tedious because within the SP approximation one must compute the electronic wave function at the centroid of each of the $O(n_{t=0}n_t)$ terms in the sum.

The resonance Raman intensity into normal mode $f$ is[70−72]

$$\sigma_R^{i\to f}(\omega_I) = C'\omega_I\omega_s^3 \left|\int_0^{\infty} \langle\phi_i|\phi_i(t)\rangle \exp(i\tilde{\omega}_I t)\mathrm{d}t\right|^2 \qquad (2.3)$$

where $C'$ is a constant, $\omega_s$ is the energy of the scattered radiation, and $|\phi_f\rangle$ is the final ground state vibrational wave function multiplied by the electronic transition dipole moment, $|\phi_f\rangle = \mu(\mathbf{R})|f\rangle$. As in the case of absorption, we assume that the Hamiltonian and (coordinate dependent) electronic transition dipole commute, and our notation (but not computation) is simplified because of the separation of time scales. We investigated both the fundamentals ($i = 0, f = 1$) and overtones ($i = 0, f = 2$) for all normal modes with and without the Condon approximation. Consider first the case of a constant electronic transition dipole. Even in this simple case the calculation of the integrand in eq 2.3, $\langle\phi_f|\phi_i(t)\rangle$, is more complicated (yet is analytic) than that of the integrand in eq 2.1, $\langle\phi_i|\phi_i(t)\rangle$. This is because $\phi_f$ is given in a normal mode coordinate system while $\phi_i(t)$ is given in a Cartesian coordinate system, and because $\phi_f$ is a product of a Hermite polynomial and a Gaussian, while $\phi_i$ involves only Gaussian functions. The matrix elements $\langle\phi_f|\phi_i(t)\rangle$ therefore require the transformation of $\phi_i(t)$ to the normal mode coordinate system at each point in time. After transforming to the normal mode coordinate frame, the problem reduces to the evaluation of (a weighted sum of) integrals that are products of correlated multidimensional Gaussians and first or second order Hermite polynomials. (The correlation arises from the transformation of the uncorrelated Cartesian time-evolving wave packet to normal modes.) These integrals are evaluated analytically using the generating function for the Hermite polynomials (see Appendix B of ref 71). Although this is a somewhat tedious procedure, it is exact and its computational cost is negligible.

When the coordinate dependence of the electronic transition dipole is taken into account, we have to rely on an approximate evaluation of the required integrals using a first-order SP approximation. Here too we must first transform the time evolving Cartesian wave function to the normal mode coordinate system. The SP approximation requires more care for the fundamental transition, since the $v = 1$ wave function is bimodal. This difficulty is overcome by expanding each of the $v = 1$ normal modes in a Gaussian basis set using one basis function for each lobe. Since two basis functions are used in each of these expansions, the number of calculations is doubled but the quality of the first-order SP approximation is greatly improved. Thus, within the SP approximation the evaluation of eq 2.3 requires for each of the (3N − 6) normal modes $O(2n_t)$ calculations of the electronic wave function. In total, at each point in time, there are $O(2n_t(3N - 6))$ calculations for the fundamental resonance Raman profile, compared to $O(n_{t=0}n_t)$ for the absorption. The effect of the coordinate dependence of the electronic transition dipole on the overtone intensities was not investigated.

## III. Results

We investigate the absorption and resonance Raman excitation profiles of ethylene following $\pi\to\pi^*$ excitation. Both excitation profiles are computed via Fourier transforms of the appropriate correlation functions (cf. eqs 2.1 and 2.3) with and without the

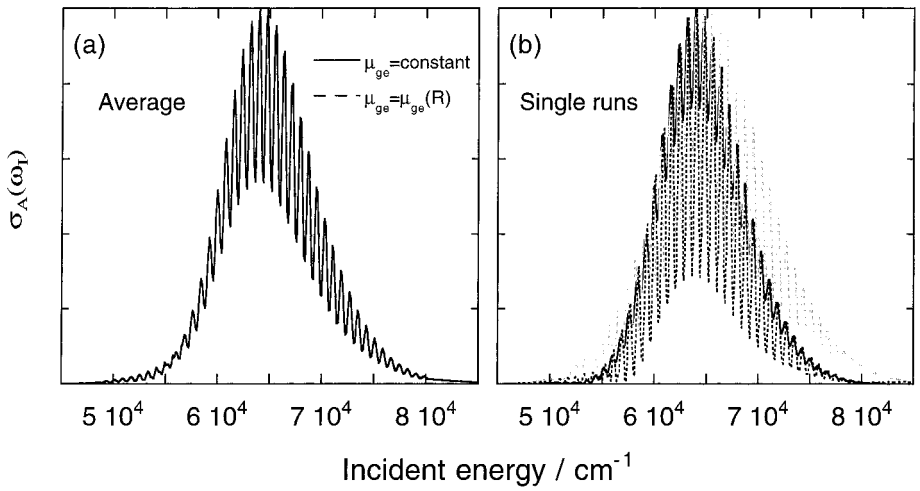


**Figure 1.** Left panel: Absorption spectrum of ethylene (intensity in arbitrary units) as a function of incident energy (in $cm^{-1}$). The results are averaged over three runs, and the absorption maximum has been shifted to coincide with the experimental value.[4] Full line: Condon approximation. Dashed line: first-order SP approximation for the time-dependent electronic transition dipole (see subsection II.D for more details). Within the SP approximation the results are indistinguishable. The width of the envelope of the absorption spectrum is $9800 \pm 1300$ $cm^{-1}$, and the recurrence in the time domain causes structure in the frequency domain spaced by $800 \pm 10$ $cm^{-1}$ (see text and Figure 2). Right panel: same as left panel but for the three individual runs within the Condon approximation. The spread in results (position and width of envelope and the extent of the high-frequency structure) is due to the truncation of the nuclear basis set.

Condon approximation. The initial position and momentum that parameterize each basis function are selected from the appropriate Wigner distribution as described in section II. C. The coupled nuclear and electronic equations of motion are integrated for 50 fs using the Runga−Kutta method with a time step of 5 atu (∼0.125 fs). At each point in time and for each nuclear basis function the multistate electronic Schrödinger equation is solved "on-the-fly" using the procedure described in subsection II. B. The derivatives of the PESs, i.e., forces, and the nonadiabatic coupling are obtained numerically using a symmetric finite difference formula with a step size of 0.005 bohr.

The extreme computational expense of ab initio multiple spawning (at each point in time $O(n_t^2 + 6Nn_t)$ potential energy evaluations are required) demands a parallelization of the propagation code. We have parallelized the code on the level of individual trajectories (i.e., basis functions) and as a consequence both the evaluation of the Hamiltonian matrix ($O(n_t^2)$ elements), and the numerical evaluation of the gradients ($6Nn_t$ PES evaluations per time step) are done in parallel. The use of parallel computing makes the simulations feasible, but not trivial. In particular, the addition of each nuclear basis function to the wave function, i.e., increasing $n_t$, results in a significant increase in computational cost. We have recently shown how this can be partially alleviated using temporally nonlocal nuclear basis functions,[50] but this has not been exploited in the simulations described here.

Ten basis functions were used to represent the initial state, and we investigated the dynamics for three different runs. These three runs differ only in the initial conditions of the basis functions. If ten basis functions were sufficient to give a complete basis set for the case in question, these three runs would provide numerically identical results. In practice, the comparison between these three runs provides an estimate for the errors due to truncation of the nuclear basis set. An alternative, and perhaps preferable, way of estimating the error would be to increase the size of the basis set. However, this is beyond our current computational capabilities.

As emphasized throughout this paper, one of our first observations is that both the absorption and resonance Raman profiles are fully determined before the onset of nonadiabatic events that bring the excited state molecule back to the ground electronic state. However, our treatment of the electronic structure assumes that the electronic excited states accessed are of predominantly valence character, i.e., the V and Z states. It is likely that nonadiabatic effects will affect the spectra when the description of other excited states is improved, particularly the lowest lying Rydberg states (through the use of diffuse electronic basis functions). Future work will investigate this possibility. Because nonadiabatic effects do not contribute to the results presented here, we do not discuss the "spawning" procedure that expands the nuclear basis set during nonadiabatic events. However, we emphasize that at each point in time we do evaluate the nonadiabatic matrix elements and we do allow the basis set to expand. (For a discussion of longer time dynamics and electronic quenching in ethylene see ref 41.)

We begin with a discussion of the absorption spectrum and of the coordinate dependence of the electronic transition dipole. The interpretation of the latter requires some analysis of the CI wave functions, which is followed by a discussion of the resonance Raman excitation profile. When possible, we compare our theoretical predictions to the experimental spectra.

Figure 1a depicts the absorption profile of ethylene computed using eq 2.1 with and without the Condon approximation (full and dashed lines, respectively). Here, and in all other figures, the absorption maximum has been shifted (by 1 eV) so that it agrees with the experimentally observed maximum.[4] The results are averaged over three runs and are practically identical with and without the Condon approximation. Thus, within the first-order SP approximation that we use for the electronic transition dipole, the Condon approximation is essentially exact (both for the averaged results and for individual runs that are not shown). This result is discussed in detail below after we conclude the analysis of the absorption profile. The width of the envelope of the absorption profile is related by the time−energy uncertainty principle to the initial decay in the overlap $\langle\phi_i|\phi_i(t)\rangle$ caused by movement of the wave function out of the Franck−Condon region. The averaged results predict a width of 9800 $cm^{-1}$, corresponding to an initial decay of the autocorrelation function within ∼1 fs. This extremely rapid motion out of the Franck−Condon region is in accord with our previous study on

ethylene,[41] where we found that the initial motion on the excited state is a fast stretching of the C═C bond. This is a consequence of the change in bond order on the excited electronic state. Within ~20 fs the C═C bond extends by >0.5 Å. This extension is significantly larger than the change in equilibrium distance between the ground and excited state, ~0.07 Å, suggesting that the excited state anharmonicity is large. As an estimate for the error arising from incompleteness of the nuclear basis set, we show in panel (b) of Figure 1 the results of the three different runs within the Condon approximation. (The results without the Condon approximation are identical and hence are not shown.) The variation in the width is ±1300 $cm^{-1}$ which is 14% of its absolute value (9800 $cm^{-1}$) and corresponds to an uncertainty of ±0.25 fs in the initial decay of the correlation function.

The experimental absorption spectrum of ethylene[1,4] exhibits a broad diffuse band and involves more than one electronic state. In particular the intense structure at the low energy end of the spectrum has been assigned to a state with predominant Rydberg character.[1] Since the computation does not include diffuse basis functions and it assumes that only the V state is accessed by the electronic excitation, it is not possible to compare (and/or reproduce) many of the experimental spectroscopic features. However, a comparison between the theoretical and experimental values for the width of the spectral envelope is possible. The experimental width of 9500 ± 500 $cm^{-1}$ reported in ref 4 is in agreement with the theoretical value of 9800 ± 1300 $cm^{-1}$. The shape of the calculated absorption spectrum does not agree with the experimentally measured one. The latter is quite skewed, tailing off slowly on the high-frequency end. Presumably, the experimental width reflects contributions from more than one electronic state (i.e., it is composed of more than one Gaussian envelope), and hence we conclude that the theoretical results (which include only one excited electronic state) are too broad.

The high-frequency structure that is superimposed on the broad envelope of the absorption spectrum is due to recurrences in the time domain. These recurrences are spaced by 42 fs (see below) and they cause a structure in the frequency domain spaced by 800 ± 10 $cm^{-1}$. This should be compared to the experimentally observed[1] spacing of 852 $cm^{-1}$. Analysis of the simulation results shows that the recurrence is dominated by the C═C stretching motion. Both individual runs (Figure 1b) and the average results (Figure 1a) show this structure, yet its magnitude varies because it depends on the extent of the recurrence, which is quite sensitive to the details of the nuclear dynamics. Compared to the experimental spectrum,[1,4] our results strongly overemphasize the structured features. For example, while our spectrum shows ~40 nonzero Franck−Condon factors, the experimental spectrum shows less than 20. If nonadiabatic effects involving the R state are important, much of this structure is expected to be washed out when a more accurate description of the electronic excited states is employed. We expect to see further reduction in the magnitude of the recurrences when the size of the nuclear basis set is increased.

The accuracy of the Condon approximation (Figure 1a) is somewhat surprising because the magnitude of the electronic transition dipole does depend very strongly on the nuclear coordinates. In Figure 2 we plot the electronic transition dipole as a function of time for a representative basis function (heavy line and right axis) and the absolute value of the autocorrelation function for one of the simulations (thin line and left axis). (The latter is very similar for the three runs.) The electronic transition dipole is certainly not constant, but rather oscillates at the excited state C═C stretching frequency and with significant amplitude

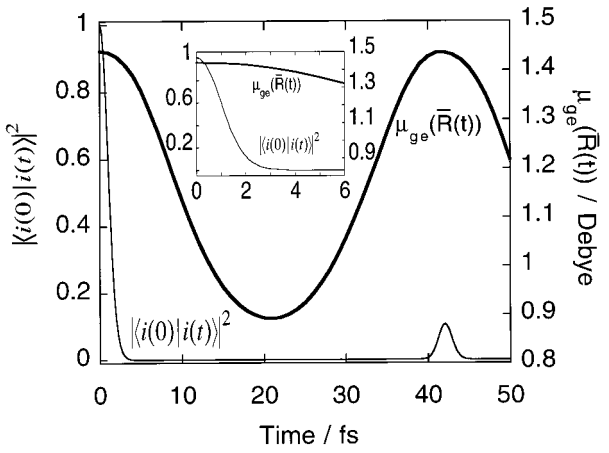


**Figure 2.** Electronic transition dipole for a representative nuclear basis function (heavy line and right axis) and absolute value of the autocorrelation function (thin line and left axis) as a function of time in fs. The inset depicts the early time behavior. The magnitude of the electronic transition dipole is dominated by oscillations in the C═C distance: as the C═C bond stretches (contracts) the electronic transition dipole decreases (increases) and these oscillations also determine the recurrence in the autocorrelation function (the bump at ~42 fs). Although the amplitude of this oscillation is large, it does not affect the autocorrelation function because the latter decays to zero within ~3 fs. As illustrated in the inset, the electronic transition dipole is nearly constant during this short time period. For the same reason the (short) recurrence at 42 fs is not affected by the time dependence of the electronic transition dipole.

(between ~1.45 and 0.9 D). As expected, the electronic transition dipole decreases when the C═C bond extends (because dissociation of ethylene results in two neutral methylene fragments) and since the latter extends by up to 0.5 Å, the decrease in the magnitude of the transition dipole is significant. However, the electronic transition dipole is nearly constant on the time scale of the decay the autocorrelation function. This is demonstrated more clearly in the inset of Figure 2 where the very short time behavior (0−6 fs) is shown. The autocorrelation function decreases to zero within 3 fs. During this time period the electronic transition dipole is practically constant. As a consequence, the Condon approximation is essentially exact and the broad envelope of the absorption spectrum is not affected by the coordinate dependence of the electronic transition dipole (Figure 1a). A similar argument explains the insensitivity of the structure in the absorption profile (which is a consequence of the recurrence in the wave function) to the Condon approximation. Approximately 42 fs after the electronic excitation, the C═C bond distance contracts back to its initial (ground state equilibrium) value and partial recurrence of the wave function is observed. When the wave function recurs, so does the magnitude of the dipole moment, and since the duration of the recurrence is very short (it increases and decreases within less than 5 fs) the electronic transition dipole is again essentially constant on this time scale.

Although the amplitude of the oscillation of the electronic transition dipole that is shown in Figure 2 is significant, the dipole does not decrease to zero. In an attempt to better understand the coordinate dependence of the electronic transition dipole, we have computed it as a function of the pyramidalization and torsion angles. The focus on these two coordinates is motivated by previous studies[73−75] of "sudden polarization." These studies have shown that pyramidalization of twisted ethylene, keeping the molecule in $C_s$ symmetry, results in a large dipole moment on the excited state with small distortions resulting in a large change in the dipole that is identically zero

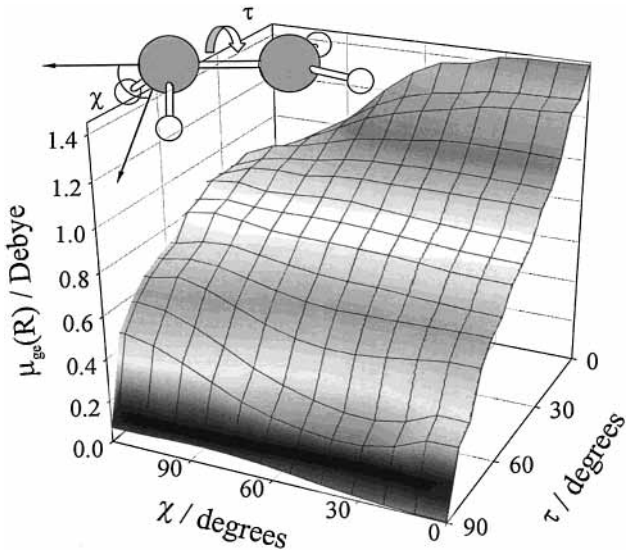


**Figure 3.** Electronic transition dipole moment as a function of pyramidalization ($\chi$) and torsion ($\tau$) coordinates. All other coordinates (bond distances and angles) are kept at their ground state equilibrium value. The pyramidalization angle is defined as the angle between the C═C axis and the bisector of the $CH_2$ plane (see sketch). At twisted geometries ($\tau = 90°$) the electronic dipole is zero (by symmetry), but at planar geometries ($\tau = 0°$) its dependence on the pyramidalization coordinate is surprisingly weak (magnitude decreases from 1.44 to 0.74 D).

at a twisted geometry. This indicates that the excited state changes its character from covalent to ionic (i.e., from V to Z), and hence it is reasonable to assume that the transition dipole will also depend strongly on these two angles.

Figure 3 depicts the electronic transition dipole as a function of the torsion and pyramidalization angles. By symmetry, the electronic transition dipole is zero at a twisted geometry. The surprising result is the somewhat weak dependence of the electronic transition dipole on the pyramidalization coordinate. Pyramidalization of *planar* ethylene, keeping $C_s$ symmetry, results in a decrease in the magnitude of the electronic transition dipole by a factor of only ~2. The dipole does depend on this angle, but the dominant coordinate is the torsion angle. In fact, the dependence of the electronic transition dipole on the pyramidalization coordinate is similar to its dependence on the C═C stretching coordinate. To understand these results, we have analyzed the Mulliken populations of the CI wave functions on the ground and excited states as a function of pyramidalization at 0° and 90° torsion angles (planar and twisted geometries, respectively). Figure 4 shows the differences in Mulliken charges between the right and left methylene fragments. For planar ethylene (upper panel), both the ground and excited states are predominantly covalent. This implies that the excited state wave function is dominated by the V state throughout, with the Z (charge transfer) state playing only a minor role. However, it is evident that the amount of Z character does increase with pyramidalization. The transition dipole moment between the Z and N (ground) states is zero because the Z state is a double excitation. Thus, the increasing contribution of the Z state explains the decrease in the transition dipole. The decrease is not more dramatic because stabilization of the Z state requires both twisting and pyramidalization. This is made clear in the lower panel of Figure 4, which is analogous to the upper panel but for a 90° torsion angle. While the ground state behaves similarly to the planar geometry, the excited state is quite different. When the C═$CH_2$ groups are planar, the covalent V state dominates the electronic wave function. As the pyramidalization increases, the wave function first becomes more ionic (Z-like) and later becomes covalent again. The first switch in character from V-like to Z-like ($\chi \approx 20°$) is the "sudden polarization" previously observed. The second switch ($\chi \approx 90°$) is a signature of the conical intersection between the N and Z states which is the primary funnel directing population back to the ground state.[41]

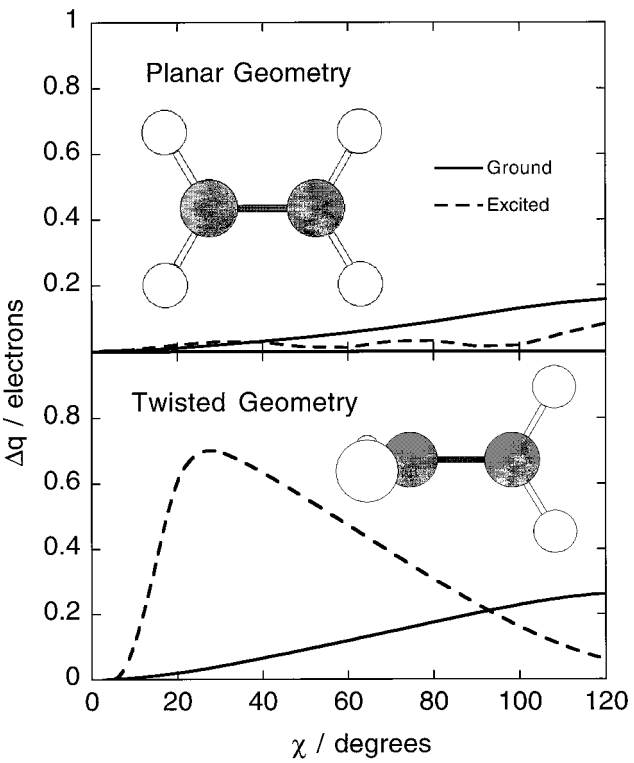


**Figure 4.** Differences in right and left methylene charges (computed using Mulliken populations for the CI wave functions) on the ground (full line) and excited (dashed line) electronic states as a function of the pyramidalization angle. Upper panel: planar geometry ($\tau = 0°$). Lower panel: twisted geometry ($\tau = 90°$). At a planar geometry (upper panel), both the ground and the excited state wave functions remain covalent as the molecule is distorted along the pyramidalization coordinate. Distortions along the pyramidalization coordinate at a twisted geometry (lower panel) result in a sudden charge separation on the excited state (fast change at small angles.)

Whereas all of these observations are relevant to the subsequent nonadiabatic dynamics, and in particular to the mechanism that brings the excited state molecule back to the ground electronic state, they do not affect the absorption spectrum because of the observed separation of time scales. The absorption spectrum is fully determined by the autocorrelation function which decays to zero very quickly (cf. Figure 2). The twist and pyramidalization angles begin to change around 30−50 fs, at which time the autocorrelation function has already decayed to zero. Consequently, we do not see any obvious signature of the torsional or pyramidalization motions in the theoretical absorption spectrum. This agrees with the original assignment by Wilkinson and Mulliken,[1] but disagrees with subsequent reassignments that have correlated the observed structure to a torsional progression.[2,3,44,45] We are currently investigating whether more accurate treatment of the Rydberg states and/or more extensive accounting of electron correlation effects will change this assignment, as well as the effect of the limited size of the nuclear basis set.

We now proceed to discuss the resonance Raman excitation profile of ethylene. We have calculated both the fundamental and the first, second, and fourth overtone resonance Raman

**TABLE 1: Character and Frequencies of the Ground State Vibrational Modes of Ethylene**

| symmetry | mode | description | computed freq ($cm^{-1}$)[a] | exptl freq ($cm^{-1}$)[4] |
|---|---|---|---|---|
| $a_g$ | 1 | $CH_2$ *s* stretch | 3331 | 3022 |
| | 2 | C═C stretch | 1733 | 1625 |
| | 3 | $CH_2$ *s* scissors | 1428 | 1344 |
| $a_u$ | 4 | torsion | 1081 | 1026 |
| $b_{1u}$ | 5 | $CH_2$ *s* stretch | 3311 | 2989 |
| | 6 | $CH_2$ scissors | 1619 | 1444 |
| $b_{2g}$ | 7 | $CH_2$ wag | 956 | 940 |
| $b_{2u}$ | 8 | $CH_2$ *a* stretch | 3424 | 3105 |
| | 9 | $CH_2$ rock | 903 | 826 |
| $b_{3g}$ | 10 | $CH_2$ *a* stretch | 3396 | 3083 |
| | 11 | $CH_2$ rock | 1347 | 1222 |
| $b_{3u}$ | 12 | $CH_2$ wag | 973 | 949 |

[a] Computed frequencies are not subjected to any scaling.

excitation profiles using eq 2.3. The validity of the Condon approximation was studied only for the fundamental lines, and we have not studied combination and/or hot bands.

The theoretical and experimental[4] ground state vibrational normal modes of ethylene are listed in Table 1. We follow the convention of Sension and Hudson[4] who took the *z*-axis to be along the C═C bond and the *x*-axis to be perpendicular to the molecular plane. According to Table 1, three modes should show fundamental Raman activity. These are the three totally symmetric modes: the $CH_2$ symmetric stretch ($\nu_1$), C═C stretch ($\nu_2$), and symmetric $CH_2$ scissors motion ($\nu_3$).

We first summarize the main features of the resonance Raman spectra of ethylene which was measured by Sension and Hudson.[4] All three of the totally symmetric modes are active at off-resonance excitation. As the excitation wavelength approaches resonance with the N → V transition, the intensity of the totally symmetric $CH_2$ stretching vibration decreases considerably (Sension and Hudson report that it disappears at a wavelength of 178 nm) and the intensity of the C═C stretch and the $CH_2$ scissors motion increases. No other fundamental lines are observed, and the most marked overtone is due to torsional motion ($\nu_4$). At certain excitation wavelengths, the spectrum is dominated by even quanta of torsional vibration. Overtones are also observed in both of the $CH_2$ out-of-plane wagging vibrations ($\nu_7$ and $\nu_{12}$), and these motions are also observed in combination bands. (The pyramidalization motion is a linear combination of these two normal modes.) Sension and Hudson concluded that the V state is strongly twisted around the C−C bond (due to the dominant progression of overtones involving even quanta of torsion) and that the $CH_2$ groups are probably no longer planar (due to the activity in overtones and combination bands of out-of-plane wagging vibrations). These conclusions about the structure of the excited state are in agreement with theoretical studies which find that, on the lowest valence excited state, the twisted geometry is a saddle point and the global minimum on this state involves pyramidalization of one of the $CH_2$ groups.[41,75]

Figure 5 depicts the resonance Raman excitation profiles (RREPs) with and without the Condon approximation (full and dashed lines, respectively) for the three totally symmetric modes: C═C stretch ($\nu_2$), $CH_2$ symmetric scissors ($\nu_3$), and the $CH_2$ symmetric stretch ($\nu_1$) (panels a, b, and c, respectively). Sension and Hudson do not report RREPs but do report the resonance Raman spectra at various excitation wavelengths. Thus, even though a quantitative comparison is not possible, we can compare the calculated spectra to the experimental results on a qualitative level. As expected, fundamental activity is found only in these three modes and the intensity of both $\nu_2$ and $\nu_3$ (panels a and b) lines is the largest. However the intensity of $\nu_1$ relative to $\nu_2$ and $\nu_3$ is too large; this line is not even observed in the experimental spectrum for wavelengths below 200 nm. A more detailed analysis of this line showed that its intensity is the most sensitive to the details of the wave function. Therefore, the error bar that is associated with this line is the largest of the three. (Note also that the largest errors in the numerical integration of the classical trajectory basis functions occur at the highest frequencies and that $\nu_1$ is a high-frequency mode. This may affect the accuracy of the wave function along high frequency modes when the nuclear basis set is small.) As in the case of the absorption profile, the high frequency structure that is superimposed on the broad envelope of the Raman profiles is due to the recurrence of the wave function on the excited electronic state (see Figures 1 and 2). Figure 5 also shows that the Condon approximation does not significantly change the results (compare the full and dashed lines). For both the C═C stretch and the $CH_2$ scissors motion (panels a and b) the Raman profiles with and without the Condon approximation are almost identical, and a nonnegligible change is observed only for the $CH_2$ stretch which as discussed above is the most sensitive. (Note that even here the change is not qualitative, i.e., the ratios between the relative intensities change by 10−20% but the cumulative effect of other errors is probably larger than this.) We can safely conclude that the effect of the Condon approximation is small when compared to other errors associated with the calculation. As for the case of the absorption spectrum, future improvements will require better electronic and nuclear wave functions and improvements of the SP approximation.

Whereas Sension and Hudson observed first overtone activity in only two of the three symmetric modes ($\nu_2$ and $\nu_3$), our calculations erroneously predict this activity in all three modes. This is perhaps expected given that our calculation also predicts the intensity of the $\nu_1$ fundamental line to be too large. In agreement with experiment we find activity in overtones corresponding to even quanta of vibration in the torsional motion ($\nu_4$), both out-of-plane wagging motions ($\nu_7$ and $\nu_{12}$) and the out-of-phase rocking vibration ($\nu_{11}$). However, the overtone of the torsion fails to dominate the spectrum, and we did not observe a progression in even quanta of the torsional vibration (i.e., the intensity of the fourth overtone is zero). Since nontotally symmetric modes derive their Raman activity through more complicated mechanisms (e.g., spreading or contraction of the wave packet), errors associated with nuclear basis set incompleteness are expected to increase. While our results fail to reproduce all of the experimental features; nevertheless, they do reproduce the features which Sension and Hudson deemed as important signatures of the excited state dynamics: pronounced activity in the C═C stretch fundamental and overtones of the torsion and out-of-plane wagging/rocking motions.

## IV. Concluding Remarks

The absorption and resonance Raman profiles of ethylene, following $\pi \rightarrow \pi^*$ excitation, were calculated from first principles molecular dynamics using the AIMS method and the correlation function formalism for molecular spectroscopy. The AIMS method provides the means for solving the electronic and nuclear Schrödinger equations simultaneously, associating a unique nuclear wave function with each electronic state. In this paper the nuclear wave function was used to construct the appropriate correlation functions, whose Fourier transforms are

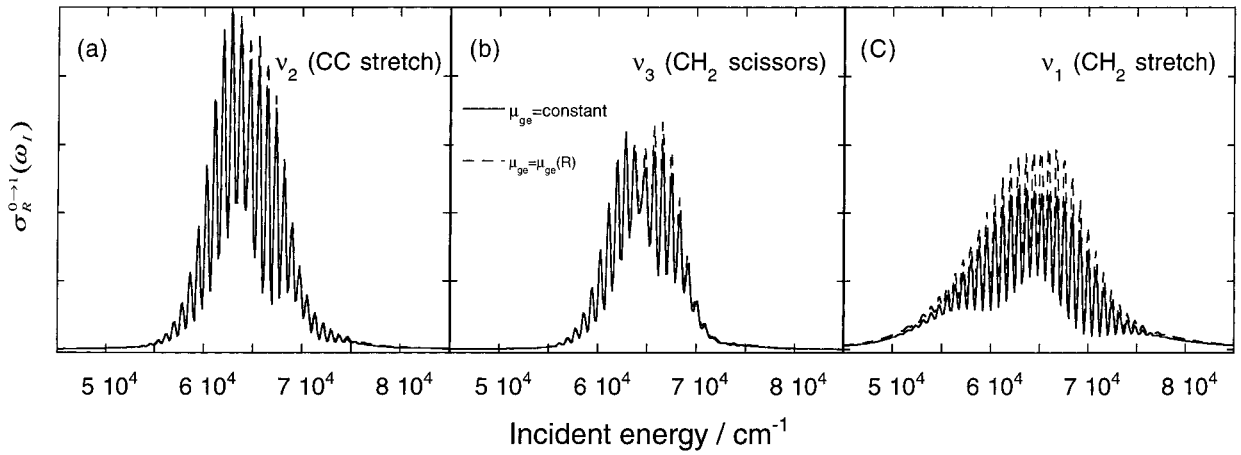


**Figure 5.** Fundamental resonance Raman intensities (in arbitrary units) as a function of incident energy (in $cm^{-1}$) for the three totally symmetric modes: C═C stretch (panel a); $CH_2$ symmetric scissors motion (panel b); and symmetric $CH_2$ stretch (panel c). The results are averaged over three runs and shifted as in Figure 1. Full line: Condon approximation. Dashed line: first-order SP approximation for the electronic transition dipole (see subsection II.E for more details). As in Figure 1 the high-frequency structure is due to the recurrence of the correlation function.

the absorption and resonance Raman excitation profiles, and the validity of the Condon approximation was investigated.

The extreme computational expense of "on-the-fly" solution of the electronic and nuclear Schrödinger equations forced us to neglect the Rydberg states. Hence only those spectroscopic features that arise due to the state with the strongest oscillator strength were modeled, and comparison to the complex experimental spectra was limited. Complete agreement with experiment is not obtained, but many of the qualitative features are correctly predicted.

We found the width of the envelope of the absorption spectrum, 9800 ± 1300 $cm^{-1}$, to be in good agreement with the experimental width,[4] 9500 ± 500 $cm^{-1}$. This width is a consequence of the extremely rapid motion of the wave function out of the Franck−Condon region and is in accord with our previous calculations[41] that showed that the initial motion on the excited electronic state is a fast stretching of the C═C bond. We found that this stretching motion is also responsible for the high-frequency structure that is superimposed on the broad envelope of the absorption spectrum. Although the predicted spacing (800 ± 10 $cm^{-1}$) is similar to that found experimentally[1] (852 $cm^{-1}$), previous interpretations have ascribed this progression to a mixture of torsional and C═C stretching motion, with the former being dominant. A discrepancy between our calculations and experiment lies in the shape of the spectrum. The envelope of the computed spectrum lacks the high-frequency tail that is observed experimentally. The origin of this disagreement is not clear. The experimental spectrum of necessity includes contributions from transitions to the Rydberg states in addition to the N→V transition on which our calculation focuses. Thus, the high-frequency tail may come from the superposition of several spectra with near-Gaussian shapes, in which case our computed spectral width is too broad. Alternatively, the approximations in our calculation (neglect of the Rydberg states and use of a limited nuclear basis set) may be responsible for the discrepancy.

As expected from symmetry considerations, the resonance Raman excitation profiles exhibit fundamental activity in the three totally symmetric modes: symmetric $CH_2$ stretching ($\nu_1$), C═C stretch ($\nu_2$), and the $CH_2$ symmetric scissors motion ($\nu_3$). The relative intensities of the last two modes are in agreement with experiment, but the relative intensity of the symmetric $CH_2$ stretch is too large. The high-frequency structure that is superimposed on the Raman profiles is similar to that observed in the absorption profile, and is again due to the recurrence of the excited state nuclear wave function (which is dominated by the C═C stretching motion). Our calculations erroneously predict overtone activity in all three of the totally symmetric modes; only two of these overtones ($\nu_2$ and $\nu_3$) are observed experimentally. In agreement with experiment, we observe even quanta of vibration in the torsional motion ($\nu_4$), out-of-plane wagging motions ($\nu_7$ and $\nu_{12}$), and the out-of-phase rocking motion ($\nu_{11}$). However, the predicted overtone activity in the torsional motion is not as intense as it should be and we did not find a progression in even quanta of the torsional vibration.

Within the first-order SP approximation used in this paper, the Condon approximation was found to be practically exact for the absorption spectrum. This is a consequence of the extremely rapid decay of the autocorrelation function, and it does not imply that the electronic transition dipole is coordinate independent. We have analyzed the coordinate dependence of the electronic transition dipole in detail, finding that it depends very strongly on the torsional coordinate and less so on the pyramidalization and C═C stretching coordinates (cf. Figures 2 and 3). However, this dependence does not affect the absorption spectrum because the electronic transition dipole is de facto constant on the time scale of the decay of the autocorrelation function (∼3 fs; see inset in Figure 2). The effect of the coordinate dependence of the electronic transition dipole on the resonance Raman excitation profile was quite small but larger than its effect on the absorption excitation profile. This is expected since the relevant overlap has to increase and decrease from zero, whereas in the case of the absorption spectrum it only decreases to zero. Hence, overall, the Raman correlation function is nonzero for a longer time period (when compared to the absorption correlation function), and as a consequence the Condon approximation is less accurate. Nevertheless, its effect is still quite small. It seems clear that the errors induced by the Condon approximation for both absorption and resonance Raman spectra of ethylene are small compared to inaccuracies in the PESs and the nuclear dynamics.

In some circles, the words "first principles" and "ab initio" are taken to imply "exact." We feel this is a misleading identification. The spectra presented here *are* generated from first principles (apart from a shift of the spectrum, there are no empirical parameters). However, we do not obtain quantitative agreement with experiment. As the experimental spectra are well known, any points of disagreement here must be resolved in

favor of experiment. By identifying and highlighting the disagreements in this paper, we hope to better characterize the weak points of our method. There are two possible directions where the calculations can be improved: the nuclear basis set and the electronic wave function ansatz. The nuclear basis set we use is far from complete and may not be adequate. The importance of Rydberg basis functions and electron correlation in the electronic structure problem is well established, and the computation of the vertical excitation energy of ethylene has occupied quantum chemists for several decades.[7,44,57,58,62,64,76−78] Practical considerations led us to exclude Rydberg basis functions, and this may have a significant effect on the computed spectra, even for the N→V transition. Future work will investigate the degree to which each of these improvements is needed to obtain quantitative agreement.

As this is the first attempt to compute an electronic spectrum using ab initio molecular dynamics, one should not be surprised at the lack of quantitative agreement. We would instead like to emphasize the qualitative agreement that is obtained, especially concerning the features of the spectrum that have been most important in deducing the early motion on the excited state.[4] There is considerable intensity in the C═C stretch fundamental, and significant overtone intensity is observed corresponding to torsional and $CH_2$ pyramidalization motion. This suggests that these three motions play an important role in the early time dynamics on the V electronic state of ethylene, as we have previously concluded in an earlier investigation of the V state photochemistry.[41]

**Acknowledgment.** It is a pleasure to dedicate this article to Kent Wilson whose vision of the role molecular dynamics should play as a tool to understand chemistry has inspired us both. This work was supported in part by the National Institutes of Health (PHS-5-P41-RR05969), the National Science Foundation (NSF-CHE-9733403), and U.S. Department of Energy (through the University of California under subcontract number B341494). T.J.M. is grateful to the NSF, Research Corporation, Beckman Foundation, and Sloan Foundation for their support through a CAREER award, Research Innovation award, Beckman Young Investigator award, and Sloan fellowship, respectively.

## References and Notes

(1) Wilkinson, P. G.; Mulliken, R. S. *J. Chem. Phys.* **1955**, *23*, 1895.
(2) Foo, P. D.; Innes, K. K. *J. Chem. Phys.* **1974**, *60*, 4582.
(3) McDiarmid, R.; Charney, E. *J. Chem. Phys.* **1967**, *47*, 1517.
(4) Sension, R. J.; Hudson, B. S. *J. Chem. Phys.* **1989**, *90*, 1377−1389.
(5) Ryu, J.; Hudson, B. S. *Chem. Phys. Lett.* **1995**, *245*, 448.
(6) Siebrand, W.; Zerbetto, F.; Zgierski, M. Z. *Chem. Phys. Lett.* **1990**, *174*, 119.
(7) Mebel, A. M.; Y.−T., C.; Lin, S.−H. *J. Chem. Phys.* **1996**, *105*, 9007.
(8) Reimers, J. R.; Wilson, K. R.; Heller, E. J. *J. Chem. Phys.* **1983**, *79*, 4749.
(9) Berens, P. H.; Wilson, K. R. *J. Chem. Phys.* **1981**, *74*, 4872.
(10) Yamaguchi, Y.; Osamura, Y.; Goddard, J. D.; Schaefer, H. F. *A New Dimension to Quantum Chemistry: Analytic Derivative Methods in Ab Initio Electronic Structure Theory*; Oxford University Press: Oxford, 1994.
(11) Fogarasi, G.; Pulay, P. *Annu. Rev. Phys. Chem.* **1984**, *35*, 191.
(12) Hudson, B. S.; Markham, L. M. *J. Raman Spectrosc.* **1998**, *29*, 489.
(13) Garavelli, M.; Negri, F.; Olivucci, M. *J. Am. Chem. Soc.* **1999**, *121*, 1023.
(14) Handy, N. C.; Gaw, J. F.; Simandiras, E. D. *J. Chem. Soc., Faraday Trans.* **1987**, *83*, 1577.
(15) Heller, E. J. *Acc. Chem. Res.* **1981**, *14*, 368.
(16) Schinke, R. *Photodissociation Dynamics*; Cambridge University Press: Cambridge, 1993.
(17) Heather, R.; Metiu, H. *J. Chem. Phys.* **1989**, *90*, 6903.
(18) Hartke, B. *J. Raman Spectrosc.* **1991**, *22*, 737.
(19) Simoni, E.; Reber, C.; Talaga, D.; Zink, J. I. *J. Phys. Chem.* **1993**, *97*, 12678.
(20) Hammerich, A. D.; Manthe, U.; Kosloff, R.; Meyer, H.-D.; Cederbaum, L. S. *J. Chem. Phys.* **1994**, *101*, 5623−5646.
(21) Tang, S. L.; Imre, D. G.; Tannor, D. *J. Chem. Phys.* **1990**, *92*, 5919.
(22) Ashkenazi, G.; Kosloff, R.; Ruhman, S.; Tal-Ezer, H. *J. Chem. Phys.* **1995**, *103*, 10005.
(23) Flothmann, H.; Beck, C.; Schinke, R.; Woywod, C.; Domcke, W. *J. Chem. Phys.* **1997**, *107*, 7296.
(24) Guo, H.; Lao, Q.; Schatz, G. C.; Hammerich, A. D. *J. Chem. Phys.* **1991**, *94*, 6562.
(25) Ramakrishna, M. V. *J. Chem. Phys.* **1990**, *93*, 3258.
(26) Qian, J.; Tannor, D. J.; Amatatsu, Y.; Morokuma, K. *J. Chem. Phys.* **1994**, *101*, 9597.
(27) Stevens, J. E.; Jang, H. W.; Butler, L. J.; Light, J. C. *J. Chem. Phys.* **1995**, *102*, 7059.
(28) Zanni, M. T.; Batista, V. S.; Greenblatt, B. J.; Miller, W. H.; Neumark, D. M. *J. Chem. Phys.* **1999**, *110*, 3748.
(29) Raab, A.; Worth, G. A.; Meyer, H.-D.; Cederbaum, L. S. *J. Chem. Phys.* **1999**, *110*, 936.
(30) Car, R.; Parrinello, M. *Phys. Rev. Lett.* **1985**, *55*, 2471.
(31) Hartke, B.; Carter, E. A. *Chem. Phys. Lett.* **1992**, *189*, 358.
(32) Leforestier, C. *J. Chem. Phys.* **1978**, *68*, 4406.
(33) Maluendes, S. A.; Dupuis, M. *Int. J. Quantum Chem.* **1992**, *42*, 1327.
(34) Remler, D. K.; Madden, P. A. *Mol. Phys.* **1990**, *70*, 921.
(35) Ben-Nun, M.; Martínez, T. J. *J. Chem. Phys.* **1998**, *108*, 7244.
(36) Ben-Nun, M.; Martínez, T. J. *J. Phys. Chem.* **1999**, in press.
(37) Martínez, T. J. *Chem. Phys. Lett.* **1997**, *272*, 139.
(38) Martínez, T. J.; Levine, R. D. *J. Chem. Phys.* **1996**, *105*, 6334.
(39) Thompson, K.; Martínez, T. J. *J. Chem. Phys.* **1998**, *110*, 1376.
(40) Martínez, T. J.; Levine, R. D. *Chem. Phys. Lett.* **1996**, *259*, 252.
(41) Ben-Nun, M.; Martínez, T. J. *Chem. Phys. Lett.* **1998**, *298*, 57.
(42) Ling, S.; Imre, D. G.; Heller, E. J. *J. Phys. Chem.* **1989**, *93*, 7107.
(43) Talaga, D. S.; Zink, J. I. *J. Phys. Chem.* **1996**, *100*, 8712.
(44) Buenker, R. J.; Peyerimhoff, S. D. *Chem. Phys.* **1976**, *9*, 75−89.
(45) Mulliken, R. S. *J. Chem. Phys* **1977**, *66*, 2448−2451.
(46) Merer, A. J.; Mulliken, R. S. *Chem. Rev.* **1969**, *69*, 639.
(47) Martínez, T. J.; Ben-Nun, M.; Levine, R. D. *J. Phys. Chem.* **1996**, *100*, 7884.
(48) Martínez, T. J.; Ben-Nun, M.; Levine, R. D. *J. Phys. Chem.* **1997**, *101*, 1A, 6389.
(49) Martínez, T. J.; Levine, R. D. *J. Chem. Soc., Faraday Trans.* **1997**, *93*, 940.
(50) Ben-Nun, M.; Martínez, T. J. *J. Chem. Phys.* **1999**, *110*, 4134.
(51) Heller, E. J. *J. Chem. Phys.* **1981**, *75*, 2923.
(52) Lengsfield, B. H., III; Yarkony, D. R. *Adv. Chem. Phys.* **1992**, *82*, 1.
(53) *Gaussian Basis Sets for Molecular Calculations*; Huzinaga, S., Ed.; Elsevier: Amsterdam, 1984.
(54) van Veen, E. H. *Chem. Phys. Lett.* **1976**, *41*, 540−543.
(55) Johnson, K. E.; Johnston, D. B.; Lipsky, S. *J. Chem. Phys.* **1979**, *70*, 3844−3858.
(56) McDiarmid, R. *J. Phys. Chem.* **1980**, *84*, 64−70.
(57) Brooks, B. R.; Schaefer, H. F. *J. Chem. Phys.* **1978**, *68*, 4839.
(58) McMurchie, L. E.; Davidson, E. R. *J. Chem. Phys.* **1977**, *67*, 5613.
(59) Bender, C. F.; Dunning, T. H., Jr.; Schaefer, H. F., III; Goddard, W. A.; Hunt, W. J. *Chem. Phys. Lett.* **1972**, *15*, 171.
(60) Evleth, E. M.; Sevin, A. *J. Am. Chem. Soc.* **1981**, *103*, 7414−7422.
(61) Petrongolo, C.; Buenker, R. J.; Peyerimhoff, S. D. *J. Chem. Phys.* **1982**, *76*, 3655.
(62) Davidson, E. R. *J. Phys. Chem.* **1996**, *100*, 6161.
(63) Garcia, V. M.; Caballol, R.; Malrieu, J. P. *Chem. Phys. Lett.* **1996**, *261*, 98.
(64) Muller, T.; Dallos, M.; Lischka, H. *J. Chem. Phys.* **1999**, *110*, 7176.
(65) Heller, E. J. *J. Chem. Phys.* **1975**, *62*, 1544.
(66) Davis, M. J.; Heller, E. J. *J. Chem. Phys.* **1984**, *80*, 5036.
(67) Heller, E. J. *J. Chem. Phys.* **1978**, *68*, 2066.
(68) Heller, E. J. *J. Chem. Phys.* **1978**, *68*, 3891.
(69) Dormans, G. J. M.; Groenenboom, G. C.; Buck, H. M. *J. Chem. Phys.* **1987**, *86*, 4895−909.
(70) Lee, S.-Y.; Heller, E. J. *J. Chem. Phys.* **1979**, *71*, 4777.
(71) Tannor, D. J.; Heller, E. J. *J. Chem. Phys.* **1982**, *77*, 202.
(72) Heller, E. J.; Sundberg, R. L.; Tannor, D. *J. Phys. Chem.* **1982**, *86*, 1822.

(73) Salem, L.; Bruckmann, P. *Nature* **1975**, *258*, 526−528.
(74) Bonacic-Koutecky, V.; Bruckmann, P.; Hiberty, P.; Koutecky, J.; Leforestier, C.; Salem, L. *Angew. Chem., Int. Ed. Engl.* **1975**, *14*, 575.
(75) Brooks, B. R.; Schaefer, H. F., III *J. Am. Chem. Soc.* **1979**, *101*, 307−311.
(76) Cave, R. J. *J. Chem. Phys.* **1990**, *92*, 2450−2456.
(77) Bender, C. F.; Dunning, T. H., Jr.; Schaefer, H. F., III.; Goddard, W. A., III.; Hunt, W. J. *Chem. Phys. Lett.* **1972**, *15*, 171−178.
(78) Dunning, T. H., Jr.; Hunt, W. J.; Goddard, W. A., III. *Chem. Phys. Lett.* **1969**, *4*, 147−150.